TITLE OF THE INVENTION

"HYPERBARIC RESUSCITATION SYSTEM AND METHOD"

INVENTORS: VAN METER, M.D., Keith, W., a US citizen, of 17 Carriage Lane, New Orleans, LA, 70114, US; and KRIEDT, Frederick, A., a US citizen, of 560 Lynnmeade Road, Gretna, LA 70056, US

CROSS-REFERENCE TO RELATED APPLICATIONS

Incorporated herein by reference are the following patent applications: co-pending US Patent Application Serial No. 09/108,464, filed 1 July 1998, which is a continuation-in-part of US Patent Application Serial No. 08/812,368, filed 5 March 1997, which is a continuation-in-part of US Patent Application Serial No. 08/348,555, filed 1 December 1994.

STATEMENT REGARDING FEDERALLY SPONSORED RESEARCH OR DEVELOPMENT

Not applicable

REFERENCE TO A "MICROFICHE APPENDIX"

Not applicable

BACKGROUND OF THE INVENTION

1. Field of the Invention

The present invention relates to hyperbaric chambers and medical treatment methods and systems using hyperbaric chambers. More particularly, the present invention relates to a system and method for using a hyperbaric chamber, a spectrophotometer (preferably a NIRoscope), and an automatic regulating device which receives information from the spectrophotometer to increase the amount of oxygen which gets to the brain of a patient being resuscitated after suffering from, for example, myocardial infarction or cerebral ischemia. The NIRoscope can also be used independently in critical care to monitor aa_3 redox ratio or even be broadened to other chromophores in the brain in conjunction with neurology and mental health.

2. General Background of the Invention

Shrinking health care dollars have made the medical profession acutely aware of the enormous cost associated with successful cardiopulmonary resuscitations. (1, 2 - the parenthetical reference numerals indicate the appropriate article listed in the Appendix). The

major expense is related to post-resuscitative care in the hospital, especially the time spent in intensive care. Cost per resuscitation depends on the percentage of survival to hospital discharge and ranges from $550,000 for 0.2% survival to $110,000 for a 10% survival. From a cost analysis perspective, it would be extremely beneficial if the number of survivors could be increased, if their post-resuscitation condition still permitted them to function as independently as possible, and if the post-resuscitation time they spent in the intensive care unit was markedly reduced. For example, it has been shown that by raising the resuscitation success ratio from the present 12% to 20%, there could be a cost savings of approximately $40,000 per patient.(2) According to Virtis (1), of the 3,308,000 patients hospitalized annually, about 1% (330,800) experienced cardiac arrest and were administered CPR. If the current success rate of 12.8% (3) could be raised to 20%, a national health care cost savings of $1.32 billion ($40,000 X 330,000) per year could be realized.

Although oxygen is considered to be the most important drug used in resuscitation from cardiopulmonary arrest, it is disheartening to learn that for the past 30 years there has been little improvement in resuscitative techniques and that advances in oxygen delivery have not been incorporated to any meaningful extent in resuscitation.

Currently, there are at least two major limitations associated with conventional oxygen delivery: the first pertains to methods of oxygen administration and the second pertains to the unavailability of a reliable, non-invasive, direct or indirect cerebral cortical oxygen monitor that could help assure adequate oxygenation of the brain during CPR. Even under ideal conditions, neither masks nor endotracheal tubes--the techniques currently used for delivering oxygen during resuscitation--deliver sufficient oxygen at sea level (1 atmosphere absolute (atm abs)) for adequate, let alone optimum, oxygen delivery. Therefore, maximum benefit, i.e. maximum recovery of cerebral neurons (minimum residual brain damage) is not attained and, thereby, represents the preeminent reason for the aforementioned dismal results with respect to minimizing brain damage following resuscitation from cardiopulmonary arrest.

What is needed is a system that will provide sufficient oxygen delivery and a sensor for non-invasively measuring in real-time the adequacy of oxygen delivery to the cortical neurons. Hyperbaric oxygen (HBO) provides the means whereby sufficient oxygen could be delivered to the patients. HBO increases the amount of oxygen physically dissolved in the plasma to an extent that greatly supplements that which is carried by hemoglobin in the red blood cells. More

importantly, HBO provides for a high partial pressure of oxygen--greater than that which could be attained at sea level--which increases the rate of diffusion of the oxygen into the tissues and cells and helps assure sufficient oxygen to overcome hypoxia and maintain cellular metabolism and integrity. It is this state of oxidative metabolism that lends itself to non-invasive measurement and, thereby, by inference, of adequate tissue and cellular oxygenation. Oxygen also exerts other beneficial physiologic-pharmacologic effects which will prevent or ameliorate the onset of hypoxia-induced cerebral and cardiac pathology.

Increasing the partial pressure of oxygen inhaled during resuscitative procedures (pressures of oxygen that can be obtained only by hyperbaric oxygen therapy (HBOT)) is expected to be pivotal in improving the success ratio of resuscitation. Such anticipation is to be expected because of the documented beneficial effects of HBOT:

1. HBOT has been suggested as an indicator for identifying potentially good resuscitative candidates. Holbach (4) reported that if patients with cerebral ischemic damage responded well to an initial exposure to HBOT they would continue to improve during post-resuscitative efforts. Patients who did not respond well to the initial HBOT exposure were less likely to recover from ischemic damage.
2. Even after extended periods of cerebral ischemia, resuscitation may be improved by HBOT (5, 6)
3. HBOT, when used in conjunction with single photon emission computed tomography (SPECT)(7, 8) using an appropriate radioactive tracer has been shown to help detect the extent of brain injury, identify if there is potentially recoverable brain tissue, and help identify the endpoint of therapy. HBOT is absolutely essential for recovering these neurons.

To effect successful resuscitations the oxygen dosage must be optimized. Holbach et al. reported that injured brain responds differently to increased pressures of oxygen than does non-injured brain. These investigators demonstrated, based on regional energy utilization, that 1.5 atmospheres absolute (atm abs) of oxygen is optimum for treating injured brain. However, Holbach was not working with resuscitation procedures in which developing and maintaining sufficient cerebral perfusion is critical for delivering oxygen and nutrients to the neurons and for removing end products of metabolism if a successful resuscitation is to be effected.

In injured brain there may be damage to the cerebral circulation thereby disrupting cerebral perfusion. The major limitation of conventional cardiopulmonary resuscitation is the failure to be able to attain and maintain a sufficient cerebral perfusion so as to sustain cardiac and neuronal function.

HBOT represents the most efficient means of supplying sufficient oxygen to tissues (neurons in the brain) thereby reversing hypoxia, sustaining neuronal metabolism, quenching free radicals, decreasing the local formation of acidosis, and stimulating angiogenesis (9). There is no drug currently available that can do what oxygen does in enhancing the survival of injured neurons (10).

It is the contention of the present inventors that real-time monitoring of cellular oxidative states, an indirect but more meaningful measure of tissue oxygen tensions, would help predict whether salvageable tissues are present. Indeed, Sheffield showed that measuring tissue oxygen tensions has been used successfully as a means for predicting which problem wounds would respond to HBOT. Not only does this technique provide predictive value, it also permits following the course of therapy so as to gauge the efficacy of the therapeutic recovery techniques. Thus, from a comparative perspective with respect to the brain, measuring cerebral partial pressure of oxygen (PO_2) during resuscitation would be an excellent gauge of successful resuscitative efforts. Waxman et al. used the PO_2 in the muscles of the upper arm to judge the success of resuscitation from hypovolemic shock (10). Rivers (11) measured cardiac venous PO_2 to predict the return of spontaneous circulation while McCormick (12) measured cerebral venous PO_2 to gauge recovery of comatose patients in intensive care. Unfortunately, no one has yet determined what is the real-time, optimal cerebral oxygen tension for tissue recovery, nor does anyone know, using current technology, how to assure that there is optimal oxygen delivery during resuscitation.

Although cerebral neurons are extremely vulnerable to hypoxia, irrespective of its etiology, there have been no reports of direct measurements of cerebral neuronal oxidative states as a means for predicting success of resuscitative efforts. One of the most important reasons for the lack of such knowledge is the absence of reliable, non-invasive instrumentation for measuring cerebral neuronal oxidation-reduction states in humans.

Based on a review of the literature, the present inventors have come to believe that the most promising approach for the non-invasive measurement of cerebral oxidation-reduction

states (cerebral PO_2) in humans is one based on near infrared (NIR) spectroscopy. Measuring the ratio of cerebral arterial and venous hemoglobin using NIR spectroscopy has been accomplished while individuals were breathing air under 1 atm abs conditions. However, this technology cannot be used under HBOT conditions because the hemoglobin in both the arterial and venous circulations may be completely saturated with oxygen. Instrumentation for measuring the in vivo cytochrome oxidase redox ratio was used successfully in bloodless small animals. (13, 16) However, attempts to apply this technology to blood-profused large animals and humans, Matcher provided inconsistent results. It has been reported the failure to obtain consistency was due to the requirement for a higher gain to detect the cytochrome oxidase redox ratio - there is less cytochrome oxidase than hemoglobin per unit volume of brain tissue and its NIR absorption signal is weaker. It appears that one of the basic problems to be overcome in applying NIR spectroscopy as an aid in resuscitating adult humans is to be able to measure the relatively weak cytochrome oxidase absorption in the presence of a pulsating hemoglobin signal that is 10 times stronger. The effects of varying Hb absorbance, water concentration and tissue light scattering have led to questionable results. (20, 21).

One desideratum for improving resuscitative efforts is a non-invasive instrument with sufficient sensitivity to measure the adequacy of tissue oxygen delivery in real-time at the cellular level so that attending physicians could optimize resuscitative efforts. Such techniques do not have to be quantitative since it is the relative changes in redox levels in real-time that are important.

Recent advances in spectroscopy have made it feasible for appropriate instrumentation to be developed. For example, charged couple device (CCD) spectrophotometers have become more sensitive and can provide absorbance spectra with integration time ranging from 10 msec to 10 seconds. This alone may be adequate to monitor aa3. If not, based on mathematical models using Fourier Transform and deconvolution methods in conjunction with data obtained from a CCD in the near infrared range, the present inventors concluded that an even more sensitive spectrophotometer could be built. In fact, by applying the inventors' algorithm to synthetic (but realistic) cerebral cortex absorption spectra, the redox ratio of cytochrome oxidase can be extracted from the spectra. Furthermore, the result of this analysis shows the real component of the Fourier Transform to be linear to the cytochrome oxidase redox ratio to the fifth decimal place. Such sensitivity should provide the basis for designing instrumentation that

is needed for making the necessary measurements of oxidized-reduced cytochrome oxidase ratios in real-time during cardiopulmonary resuscitation. This same technique may be applied to other natural chromophores in the brain such as neuron transmitters or treatment drugs in conjunction with the diagnostics treatment of neurology and psychiatry.

Hyperbaric chambers have long been used for increasing the amount of oxygen supplied to patients suffering from oxygen deprivation. Several articles and patents address this subject. However, it is important to supply the proper amount of oxygen to a patient. Supplying too much can be almost as harmful as supplying too little.

U.S. Patent Nos. 3,688,770, 3,877,427, and 3,547,118 disclose hyperbaric chambers for oxygenating blood. In U.S. Patent No. 3,547,118, a regulator automatically controls the relationship between the pressure of the chamber and the pressure of the oxygen supply of a patient in the chamber. U.S. Patent No. 4,582,055 discloses a similar system.

U.S. Patent No. 5,220,502 discloses a system for automatically measuring the blood pressure of a patient in a hyperbaric chamber.

U.S. Patent Nos. 4,281,645; 5,313,941; and 5,873,821 disclose spectrophotometers.

U.S. Patent Nos. 3,984,673, 4,448,189, and 4,633,859, disclose various apparatus for controlling the environment in hyperbaric chambers.

See also Dalago et al., SU patent document no. 395,091, December 1973; F.G. Hempel et al., "Oxidation of cerebral cytochrome aa3 by oxygen plus carbon dioxide at hyperbaric pressures,": J. Applied Physiology: Resp.; Env., and Exercise Phys., Vol. 43, No. 5 (11/1977); and S.D. Brown et al., "In vivo binding of carbon monoxide to cytochrome c oxidase in rat brain," J. Applied Physiology, Vol. 68, No. 2 (2/1990); and U.S. Patent No. 5,251,632.

All references mentioned herein (and all references to which they refer) are hereby incorporated herein by reference.

BRIEF SUMMARY OF THE INVENTION

The present invention is a hyperbaric resuscitation method and system including a hyperbaric chamber and a spectrophotometer; the system includes means for automatically regulating the amount of oxygen in the gas breathed by the patient by regulating the oxygen concentration and pressure of the breathed gas using information from the spectrophotometer.

The method of the present invention comprises placing a patient in a hyperbaric chamber having a volume sufficient to enclose a human patient and at least two operating personnel,

pressurizing the hyperbaric chamber to greater than existing barometric pressure (preferably to at least 1.5 atmospheres), providing oxygen-rich gas to be breathed by the patient via a previously placed endotracheal tube, pressurizing the oxygen-rich gas to a pressure similar to that of the hyperbaric chamber, and monitoring oxygen in cerebral tissue of the patient with a non-invasive monitoring means. The method preferably also includes the step of automatically regulating the concentration of oxygen in the oxygen-rich gas supplied to the patient via endotracheal tube in response to readings of the non-invasive monitoring means. The operating personnel breathe chamber air which is not oxygen rich.

The present invention comprises a device, the use of which will assist in real-time evaluation of the efficacy of advanced cardiac life support (ACLS) resuscitation procedures. Specifically, the present invention comprises a near infrared sensor (NIRoscope) capable of non-invasively measuring real-time changes in the oxidation-reduction (redox) states of cytochrome oxidase in the cerebral cortex of patients (adults and children) undergoing emergency cardiopulmonary resuscitation in an hyperbaric environment. The real-time changes in redox states will be used immediately by the attending physician to assess the efficacy of their resuscitative efforts and to help direct changes so as to optimize the ACLS procedures for the individual patients. The net result of these efforts should be an enhancement of procedure efficacy thus helping to assure patient survival. In addition, successful application of NIRoscope-assisted resuscitation procedures should also result in the preservation of as much functional brain tissue as possible thereby yielding an increase in patients' self-reliance and a decrease in the length of time patients are required to stay in the intensive care unit at the hospital.

As procedures are developed and stabilized, an additional improvement would be to remotely treat the patient from outside the chamber and lock in medical personnel if complications arise.

The present invention comprises a NIRoscope capable of measuring a cytochrome oxidase redox near infrared (NIR) signal with a 0.1 optical density (OD) unit total range with a 0.005 OD sensitivity in a pulsating 1.0 OD hemoglobin NIR signal. To test the present invention, measured accuracy will be evaluated by processing existing spectrum from rats, a human forearm and piglets, along with collected data from adolescent swine, adult humans and comparing the inventors' algorithm with the presently used multi-component analysis algorithms available today. Results will be compared to determine which data processing method is

superior. Testing of the instrument on an existing, on-going, acute swine model will occur at an institute under normal atmospheric and hyperbaric conditions. This testing will establish the accuracy, safety and effectiveness of the instruments by invasive techniques. Once accuracy and safety have been established, the instrument will be utilized to conduct research at a major trauma center, recording the redox ratio of cytochrome oxidase in patients undergoing emergency resuscitation. At the same time another like instrument will be incorporated into swine model resuscitation experiments on-going at the same institution. Further testing would involve a controlled human trial of resuscitation using a NIRoscope-assisted resuscitation in an hyperbaric environment.

It is an object of the present invention to provide an integrated system for non-invasively measuring cerebral neuronal oxidation-reduction states during cardiopulmonary resuscitation in an hyperbaric environment.

It is another object of the present invention to provide a NIRoscope and a new mathematical method that is used to enhance the instrument's sensitivity and ability to measure, in real-time, the change in the redox state of patients undergoing resuscitation. The NIRoscope will be tested in an existing acute animal resuscitation model and in a chronic extension of this model. Shortly thereafter, a NIRoscope will be used in a clinical setting to measure the changes in cerebral redox states during presently on-going ACLS-approved human resuscitation. It is during this preliminary clinical test that techniques for attaching the NIRoscope to the patient will be refined and knowledge will be increased about the redox behavior of the cytochrome oxidase during resuscitation. Later, a clinical study comparing standard human resuscitation with hyperbaric resuscitation will be performed.

It is also an object of the present invention to provide a resuscitation method and system including a hyperbaric chamber and a spectrophotometer;

It is a further object of the present invention to provide a resuscitation method and system including means for automatically regulating the amount of oxygen in the gas breathed by the patient by regulating the oxygen concentration and pressure of the breathed gas using information from the spectrophotometer;

It is another object of the present invention to provide a hyperbaric resuscitation system comprising a hyperbaric chamber having a volume sufficient to enclose a human patient and at least two operating personnel, means for providing oxygen-rich gas through an endotracheal tube

to be breathed by the patient, pressurizing means for pressurizing the hyperbaric chamber (preferably to at least 1.5 atmospheres) and for pressurizing the oxygen-rich gas to a pressure similar to that of the hyperbaric chamber, a spectrophotometer for monitoring oxygen in cerebral tissue of the patient, and regulating means for regulating the concentration of oxygen in the oxygen-rich gas in response to readings of the spectrophotometer.

It is another object of the present invention to provide a resuscitation method comprising an unmanned hyperbaric chamber sufficient to enclose one human patient, a means for providing oxygen rich gas to be breathed by the patient via an endotracheal tube with all ACLS devices placed and fixed to the patient before pressurization which can be operated from outside the hyperbaric chamber.

It is another object of the present invention to utilize the Niroscope's ability to non invasively monitor cerebral cortical changes in hemoglobin, water and the redox state of cytochrome oxidase, independent and without the use of HBO. The ability to observe the previous mentioned changes with the Niroscope is expected to enhance the art and science of medicine where cellular respiration is or has been impaired. Examples include the following: in neurological rehabilitation centers as a guide for improving cerebral function after local cerebral damage due to stroke, trauma, or exposure to toxic or anoxic encephalopathies, in the operating room as a guide for evaluating cerebral oxygenation status during surgery where cerebral blood flow has been compromised i.e. bypass surgery, percutaneous transluminal coronary angioplasty, or endarterectomy; in evaluating cerebral hemodynamics and oxygen utilization in fetal and neonatal brains as a guide for detecting and managing hypoxic/anoxic states irrespective of etiology; in organ donation as a guide for improved management of brain-dead organ donors; and in any area of research requiring non-invasive monitoring of changes in the function of the respiratory chain (12). It is another object of the invention to measure the change of absorbance spectra for any natural or synthetic chromophore that exist or is introduced in the brain. Examples of natural chromophores would be any neurotransmitter that has an absorbance peak in the 600 - 1050 nm range. An example of a synthetic drug would be any neurologic or psychiatric drug (lithium) that would be used by a neurologist or psychiatrist. The technique would be to establish a baseline at some certain point and monitor the change in absorbance spectrum after a given time based on patient symptoms. Symptom and absorbance spectra could be correlated by the attending physician.

BRIEF DESCRIPTION OF THE SEVERAL VIEWS OF THE DRAWINGS

For a further understanding of the nature, objects, and advantages of the present invention, reference should be had to the following detailed description, read in conjunction with the following drawings, wherein like reference numerals denote like elements and wherein:

Figure 1 shows theoretical absorption spectra excluding water expected to be found during evaluation of an adult human. The axis of abscissa is wavelength (λ) in nanometers, and the axis of ordinates is absorbance (Abs) in optical density. These curves were computer generated using published extinction coefficients in the near infrared range (Wray 1987), concentrations typically found in the brain (Cope 1988) and based on the fact that the path lengths are equal in all cases, allowing a 1 cm. value to be assumed. Each curve represents 100% oxygenated hemoglobin (hyperbaric conditions) and various percentages of oxidized cytochrome oxidase from 0% (bottom curve) to 100% (top curve).

Figure 2 shows the same absorption curves of Figure 1, with D.C. component removed by subtracting the average absorption value of the spectrum at each wave length from the original spectrum.

Figures 3, 4, and 5 are Fourier transforms of absorbance curves. Figure 3 is 0% oxidized cytochrome oxidase, Figure 4 is 50% oxidized cytochrome oxidase, and Figure 5 is 100% oxidized cytochrome oxidase. The axis of abscissa is wavenumber (N) in 1/nanometer and the axis of ordinates is the Fourier coefficient (Fo). Notice that the only component that is changing is the real component of the Fourier transform. It was found to be linear to the fifth significant place (see Figure 6).

Figure 6 is a plot of the magnitude of the first real component of the Fourier transform (axis of abscissa) versus percent oxidized cytochrome (axis of ordinate). It was found to be linear to the fifth significant figure (i.e., in this case - .017865) and therefore expected to be an extremely sensitive indicator of oxidized cytochrome oxidase.

Figure 7 is a schematic diagram of the NIRoscope of the present invention.

Figure 8 is a schematic diagram of the NIRoscope without the background signal pickup optode. The background signal is taken as reference before the sample signal is taken.

Figures 9 and 10 are side and top views, respectively, of the preferred embodiment of the apparatus of the present invention.

Figure 11 is a top view of another embodiment of the apparatus of the present invention.

Figure 12 shows the NIR light source of the present invention.

Figure 13 is a schematic view of a single point pickup unit.

Figure 14 is an illustrative view of a ring pickup unit (to optimize light collection).

Figure 15 is schematic view of a ring pickup unit.

Figure 16 is sectional schematic view of a ring pickup unit.

Figure 17 is a schematic view of a Fresnel lens pickup unit with internal light input.

Figure 18 is a schematic view of an optical arrangement of Fresnel lens pickup unit with external light input.

Figure 19 is a schematic view of an optical arrangement of a spherical mirror pickup unit with external light input.

Figure 20 shows a dual wavelength interval spectrophotometer.

Figure 21 is a diagram showing how the various features of the present invention are interconnected.

Figure 22 is a diagram showing alternate features of present unit without real time background measurement using the Fresnel pickup unit.

Figure 23 is a software logic diagram (with real time background measurement).

Figure 24 is a software logic diagram (without real time background measurement).

Figure 25 shows absorption curves for hemoglobin, water and cytochrome oxidase.

PARTS LIST:

The following is a list of suitable parts and materials for the various elements of the preferred embodiment of the present invention.

1 patient

2 patient's head

3 calculated spectrum of predicted absorbance found in a human head

4 curve of the magnitude of the Fourier transform of the absorbance spectrum versus wave number

5 spectrum 3 with DC component removed

6 curve of the real component of the Fourier transform of the absorbance spectrum versus wave number

8 curve of the imaginary component of the Fourier transform of the absorbance spectrum versus wave number

9 curve of the real component of the Fourier transform (FoR) of the absorbance spectrum versus percentage of cytochrome oxidase (% ox aa_3)

10 hyperbaric resuscitation system (directed patient access) of the preferred embodiment of the present invention

20 multiplace hyperbaric chamber

21 rolling cart in hyperbaric chamber 20

22 quick-opening closure of hyperbaric chamber 20

23 outer lock of hyperbaric chamber 20

24 wall of chamber 20

25 inside of chamber 20

26 outside of chamber 20

27 patient gurney

28 wheels for quick opening closure

31 defibrillator/cardiac monitor

32 suction equipment

33 regulator/ventilator

34 code cart

35 blood gas monitor

36 arterial blood pressure manometer

37 EKG monitor

38 rectal core thermistor

39 Thumper-Michigan CPR controls

41 breathing gas mixer

42 endotracheal tube connected to oxygen enriched breathing gas mixture

43 tunnel connecting main chamber to monoplace chamber

51 NIR oxygen monitor (inside chamber)

52 NIR oxygen monitor (outside chamber)

60 emergency personnel (doctors, nurses, et al.)

81 door

82 door

100 stabilized near infra-red light source

101 light source (e.g., Oriel 66195)
102 Lamp (e.g., 100 watt Oriel 6333)
103 Hot mirror housing
104 Visible light fiber optics adaptor (e.g., Oriel 77797)
105 Hot mirror (e.g., Andover 775 FW 82-50S)
106 Near infrared fiber optics adaptor (e.g., Oriel 77797)
107 fiber optics light conduit
108 Photo feedback system (e.g., Oriel 68850)
109 Power source (e.g., DC feedback Oriel 68830)
110 Stabilized power supply
111 Parabolic light collector
120 total light path
122 visible light path
124 NIR light path
200 Single point pickup unit
201 Light dam
202 Collimating lens beam probe (light input)
203 Collimating lens beam probe (background pickup)
204 Collimating lens beam probe (sample pickup-cerebral cortex)
205 Scalp
206 Skull
207 Dura
208 Pia
209 Arachnoid
210 Cerebral cortex
211 Multioptode ring pickup unit
212 NIR diffuse light path (background)
213 NIR diffuse light path (sample-cerebral cortex)
216 fiber optic cable for light input
218 fiber optic cable for background light
220 fiber optic cable for sample light

222 electric signal wire
224 computational and control equipment
226 optode frame with angular adjustment to light input and pickup
228 mirror lined or polished surface
230 Fresnel pickup unit
231 Fiber optics bundle (e.g., Dolan Jenner XL 536T)
232 Light dam assembly
233 Rubber boot
234 Fresnel lens (e.g., Edmond Scientific D43,012)
235 Collimating lense (e.g., Donan Jenner LH 1200)
236 Fresnel upper housing assembly
237 Fresnel lower housing assembly
250 spherical mirror pickup optode
251 optode barrel
252 encap housing
253 mirror housing
254 mirror cap
255 spherical mirror (such as Edmond Scientific part no. J43-544)
256 O-ring light seal
300 Dual wave interval spectrophotometer
301 Optical enclosed chopper (e.g., Oriel 75155)
302 Bifurcated fiber optics bundle (e.g., Oriel 77533)
303 Spectrograph (e.g., Oriel 77400)
304 Aperture
305 CCD Spectrophotometer
306 Optical grating (e.g., 600-1100nm)
307 Charge coupled device (e.g., Oriel Inter Spec IV)
308 Amplifier
309 A/D converter card
310 Interface unit
311 Personal computer

312 Data storage unit (e.g., Syquest)
313 Monitor
314 Printer
315 Clock driver timer module
316 Computational equipment
400 Signal extraction processing software (with real time background removed)
402 Real time alternating background spectra (a 6 second integration time and a 4 second interval time)
403 Real time alternating sample spectra (a 6 second integration time and a 4 second interval time)
404 Averaging sub routine
405 Sav-Golay 2nd degree polynomial with 51 points subroutine
406 Fourier window (wave length interval) specified (for Hb, HbO, H2O, and cytochrome oxidase)
407 DC signal removed by subtracting average absorbance from actual value
408 Fourier transform analysis subroutine
409 Fourier deconvolution analysis subroutine
410 Result stored
411 Corrections summed
412 individual noise (cosmic) pixels corrected subroutine
413 Difference absorption spectra sub routine
415 average absorbance computed (result of integral/wavelength interval)
416 signal extracting processing hardware (without real time removal)
417 first (fundamental) real component of Fourier transform
418 real time background spectra (20 each, a 6 second integration time and a 4 second interval time)
450 absorbance curve for oxygenated hemoglobin
452 absorbance curve for de-oxygenated hemoglobin
454 absorbance curve for oxidized cytochrome oxidase
456 absorbance curve for reduced cytochrome oxidase
458 absorbance curve for water

460 correction applied to cytochrome oxidase signal

469 deoxygenated hemoglobin peak at 760 nm

500 Dual wave interval spectrophotometer

510 hyperbaric resuscitation system (remote patient access)

520 monoplace hyperbaric chamber

534 external/internal IV

539 Thumper-Michigan chest compression device

560 emergency room personnel (doctors, nurses, et al. (ready to provide patient with direct access))

611 exit ring for light input

620 hyperbaric chamber (such as a conventional hyperbaric chamber)

630 Optional Fresnel lens pickup unit

DETAILED DESCRIPTION OF THE INVENTION

In Figures 9 and 10, the preferred embodiment of the hyperbaric resuscitation system of the present invention is designated by the numeral 10.

The system is preferably composed of a hyperbaric chamber 20 with minimum dimensions of 96" (2.44 m) in diameter with a 14' (4.27 m) usable length, capable of being pressurized to four atm abs, and built to pressure vessel human occupancy (PVHO) standards. Access to the chamber 20 can be through doors 81 and 82 large enough to roll equipment and patient 1 in and out (e.g., 34" x 54" - 86cm x 137cm). Access is preferably also provided by a quick-opening closure 22 with an opening diameter equal to the diameter of the chamber 20. The entire resuscitation cart 21 will roll in and out of the chamber. The resuscitation cart comprises the patient gurney 27, floor space around the gurney 27 for two to five emergency personnel 60, a capnometer (monitor of CO2 in exhaled gas - not shown), a defibrillator/cardiac monitor 31 with intravascular pressure monitoring capability, suction equipment 32, volume cycled patient regulator/ventilator 33, American Heart Association approved code cart 34, a blood gas monitor 35, an arterial line blood pressure manometer 36, continuous EKG cardiac monitor with recorder 37, rectal core thermistor 38, x-ray equipment (not shown) for anterior/posterior neck, chest, and abdomen conventional views by portable x-ray equipment, a pulse oximeter (not shown) and a NIRoscope 51 capable of rapidly and continuously measuring cytochrome oxidase redox ratio in the cerebral cortex of the patient 1.

If one is willing to forego the quick-opening closure 22, one could use a standard hospital hyperbaric chamber commercially available from Perry Oceonographics Company.

All NIRoscope-related equipment on the resuscitation cart 21 must be checked for suitability for operation in an hyperbaric atmosphere and, if necessary, the requisite modifications must be made. All above equipment is installed on a cart capable of being moved in and out of the entrance doors 81/82 of hyperbaric chamber 20.

The method of the present invention comprises placing a patient 1 with endotracheal tube 42 in place into hyperbaric chamber 20 having a volume sufficient to enclose a human patient 1 and at least two operating personnel 60, pressurizing the hyperbaric chamber 20 to greater than existing barometric pressure (preferably to at least 1.5 atmospheres), providing oxygen-rich gas to be breathed by the patient 1 through endotracheal tube 42, pressurizing the oxygen-rich gas to a pressure similar to that of the hyperbaric chamber 20, and monitoring oxygen in cerebral tissue of the patient 1 with a non-invasive monitoring means (such as NIRoscope 51, 52). The method preferably also includes the step of automatically regulating the concentration of oxygen in the oxygen-rich gas in response to readings of the non-invasive monitoring means. At the option of the emergency center/attending emergency physician, a monoplace chamber 520 can house the patient 1 and all ACLS procedures conducted from the outside of the chamber 520 by robotic design (see Figure 11). Chamber 520 is provided with a connecting tunnel 43 to chamber 620 in case patient access is needed by medical personnel 560. In such a case, medical personnel 560 would enter chamber 620, chamber 620 would be pressurized to the same pressure as chamber 520, then the personnel 560 would enter chamber 520 to work with patient 1.

Description of Present Niroscope Algorithm Technology - Multi-Component Analysis (MCA)

Niroscopy is the application of absorption spectroscopy in the near infrared range for measuring the change in concentration of specific chromophores. The primary chromophores that are designated for measurement are oxidized and reduced cytochrome oxidase and oxygenated and deoxygenated hemoglobin.

Currently, measuring the change of the concentration of these chromophores by niroscopy is based on the following considerations and procedures. Given an absorption curve over a range of wave lengths in the near infrared region (700 - 950 nm) and assuming Beer's law is applicable, a set of simultaneous equations can be generated which, when solved, will result in concrete values for the relative concentrations of each of the chromophores. The number of equations is

equal to the number of chromophores whose concentrations are to be determined. For example, in the brain, for the near infrared spectral region, there are the four aforementioned chromophores. If any four different near infrared wave lengths are selected for making total absorption measurements, four total absorption values will be obtained. Using Beer's law, it is possible to solve for the concentration of each of the chromophores. The equations that are generated will contain the following variables: total absorption, chromophore extinction coefficients, concentration of each chromophore, and path length. Total absorption is obtained by direct measurement. Chromophore extinction coefficients are determined experimentally. Total path length involves a complex series of events which may be considered constant for the system and therefore can be assumed to be unity. By solving these simultaneous equations by matrix operations it is possible to calculate the relative concentrations of each of the chromophores. The ratio of oxidized and reduced cytochrome is then calculated from the values obtained from the solution of the equations.

The present method has certain errors inherent in its application. These are:

1. The method assumes Beer's law is linear. However, Beer's law is not linear in a scattered media or in the presence of large absorbance changes of other chromophores.
2. The extinction coefficients of cytochrome have been measured in bloodless rats where cytochrome oxidase was assumed to exist either entirely in the oxidized or completely reduced state. Experimental evidence has shown that a condition of total oxidation or reduction of cytochrome oxidase does not exist. Also a slight hemoglobin contamination was present during these measurements for which no correction was made. Therefore, the relative concentrations of the cytochromes that were calculated were not accurate.
3. The effects of water absorption overtones cannot be taken into account by modeling with Beer's law.
4. Because of the limitations associated with items 1 and 2, current niroscopic techniques do not permit consistent measurements in adult humans. The signal obtained in adult humans is extremely faint since it is being masked by the high hemoglobin concentration.

The present inventors perceived a need to develop niroscopic techniques that would

obviate these limitations. The following is the theoretical description of the bases of the innovation of the present invention.

It is the contention of the present inventors that the aforementioned limitations of the niroscopic techniques can be overcome by the use of a specific range of near infrared waves (600 - 1100 nm) from which the change of a single absorption curve is obtained and used directly or corrected and from which the relevant data can be extracted via model-free mathematical operations, i.e. Fourier transform/deconvolution analyses (FTA/FDA). Fourier transforms are commonly used for infrared analysis and in digital signal filtering techniques, but are not so used in analyses of near infrared data. There is no obvious theoretical reason why such analyses could not be performed on data obtained from near infrared analyses. Therefore, the present inventors decided to incorporate such analyses in theoretical models.

The data used to demonstrate our proposed Fourier transform operations are derived from a theoretical construct. A family of spectra is generated using Beer's law, and a set of measured extinction coefficients for each of the chromophores (Nioka 1991), and assuming a certain published physiological concentration of each chromophore obtained from Cope (1988) and Miyake (1991). After assuming hemoglobin is 100% oxygenated, each calculated spectrum for a specific cytochrome oxidase (cyt-aa_3) redox ratio (i.e. varying from reduced to oxidized in steps of 10% is plotted as optical density versus the wave length range of 700 to 950 nm (Figure 1)).

The cyt-aa_3 absorbance extraction is as follows. Each spectrum in the resultant family of spectra (Figure 1) is subjected to removal of the DC component by subtraction of the average (i.e. total area under each curve divided by the wave length interval), resulting in the curves shown in figure 3. The curves in figure 3 are then subjected to Fourier transform procedures. Form the results of Fourier transforms, it is observed that the only value that changes as a function of the cytochrome redox ratio is the real component in the fundamental frequency. Figure 2 shows the amplitude of this real component of the fundamental frequency is linearly proportional to the percent oxidized cytochrome oxidase (i.e. redox ratio) to the fifth significant figure (i.e. 0.04212 div./redox ratio of cyt-aa_3).

The theory of Fourier transforms (Brighan 1988) explains the reason for linearity. Figure 25 displays the absorbance for each chromophore in the 700-1100 nm wave length range. Notice that the oxidized cyt-aa_3 spectrum 454 completes one cycle (i.e. the fundamental frequency in

the 700-950 nm wave length interval). None of the other chromophores have this feature. Fourier transform operator separates out the contribution of each component harmonic. The only spectrum completing one cycle in the chosen wave length interval is oxidized cyt-aa_3. The effect is to extract the cyt-aa_3 while filtering out all other absorbance bands. Signal extraction is improved by another Fourier transform feature. When a Fourier transform is performed on a function (i.e. absorbance spectra), one real value and one imaginary value will be determined for each component frequency. The real value represents the symmetrical portion of the component frequency, and the imaginary represents the asymmetrical portion of the component frequency. For a wave length interval of 700-950 nm, cyt-aa_3 is symmetrical (i.e. only the real component is representative) which once again extracts the cyt-aa_3 absorbance peak and filters out all others. This is the reason why the real component of the fundamental frequency is significantly linearly proportional to cyt-aa_3 redox ratio.

The extraction technique is also quite robust with respect to signal to noise ratios (S/N). Calculations have shown, when reducing the S/N ratios from 45 to 1.39, the fundamental real component 468 does not change appreciably (±2%). Even when considering inexpensive, noisy spectrophotometers which have a low S/N ratio, the S/N, although low, usually remains relatively constant. It will be removed with the DC portion of absorbance spectra. This implies that as long as the signal can be extracted (i.e. not completely buried) noise will have little effect. Removing the DC component and the Fourier transform also reduces the effect of noise due to scattering.

The effects of large variations in Hb and water were studied by generating another theoretical construct of spectra (i.e., high and low concentrations for Hb and water). These spectra were processed, and the resultant real component of Fourier transfer change approximately 2%. Because our goal is to have Hb or water affect the signal by 1% or less, a second Fourier transfer tool may be required.

This second tool, Fourier deconvolution analysis (FDA) has been explained in detail by Blass (1981).The expected NIR total absorbance spectra is a combination of the major absorbance curves shown in Figure 25. Both de-oxygenated Hb 452 and reduced cytochrome oxidase 456 have spectra resembling exponential decay, except de-oxygenated Hb has a narrow peak 469 with a half width of 30 nm, centered at approximately 760 nm. The oxygenated form of hemoglobin 450 and the oxidized state of cytochrome oxidase 454 have broad peaks, with

cytochrome oxidase having a half width of 175 nm (725-900 nm) centered at 830 nm and deoxygenated hemoglobin having a halfwidth of 400 nm centered at 812 nm. Because both water and de-oxygenated Hb have distinct peaks, Fourier self-deconvolution can be applied (Blass 1981). It is a method for resolving intrinsically overlapping absorbency bands (an NIR total absorbance spectrum) into each component absorption curve of interest (de-oxygenated hemoglobin and water). It is, however, noise sensitive (i.e., will resolve noise if S/N ratios are large enough) and therefor requires an expensive (noise free) CCD spectrophotometer. If a noise free (i.e., S/N greater than 1000) spectrophotometer is used, FDA allows monitoring deoxygenated hemoglobin, and water separately. If there is a change in cyt-aa_3 absorbance inflicted by Hb or water overtones, a corresponding correction can be made to the cyt-aa_3 result. The ability to monitor cerebral edema or de-hydration (changing water content) will also be useful information and could be easily displayed separately.

A third tool called differential absorption spectroscopy may also be utilized to enhance the extraction of the cyt-aa_3 absorbance contribution. Rather than use an arbitrary reference (water for transparent spectroscopy or water plus microspheres for diffuse spectroscopy) a reference spectra is taken in vivo either at a certain time (admission of the patient) or tissue location (lower distance from light source than sample - see Figures 13, 14, or 15, probe 203). Using these spectra as reference will allow sensitivity to be increased by measuring change in absorbance rather than the actual value of absorbance.

In summary, increasing the sensitivity of measurement with differential absorption spectroscopy and by combining the accurate measurement of FTA with the possible correction to the cyt-aa_3 measurement made by FDA, we can non-invasively measure the change in the cyt-aa_3 redox ratio with a model-free analysis using standard digital signal conditioning techniques. This should result in improved accuracy in adolescent swine and ultimately in the adult human head.

Data Handling Requirements

The preferred equipment (see Fig. 5) comprises a near infra-red light source 100, an optical pickup unit 211, and dual wave interval spectrophotometer 300, and computational equipment 316.

Near infra-red light source 100 (see Fig. 12) is preferably a 100 watt power light source 101 in a steady or pulsating mode (frequency range .5 - 2 Hz). An example of a suitable unit

would be Oriel 100 watt quartz halogen light source with DC stabilized radiometric power supply, including photofeedback system, water filter, multiple filter holder/fiber optic adaptor (Oriel model numbers 66195, 68850, 61940, 62020 and 77797).

Optical pickup unit 200/211 (see Figs. 13,14, 15, 17, 18, 19) consists of fiber optics light conduit 231connected to a single or ring of collimating beam probes 202 which inputs the light. The background light receivers are recessed single or ring collimated beam probes 203 adjusted at the proper angle to received background light. The sample light is again a recessed single collimated beam probe 202 either at the center of the rings (Fig. 15 and 16) or in single operation adjusted at the proper angle to receive light input (Fig. 13) (Oriel model 77545 and 77645). It should be noted that if the signal separation is satisfactorily accurate, subtraction of the background signal will not be necessary thereby eliminating the need for 16 each background pickup optodes 203, optical chopper 301, and bifurcated fiber optics bundle 302. The preferred alternate equipment schematic is shown in Figure 8.

Dual wave interval spectrophotometer 300 consists of an optical chopper 301, bifurcated bundle 302, and CCD spectrophotometer with sensitivity adequate to measure .005 O.D. absorbance and a dynamic range capable of measuring 4 O.D. in a wave length range of 600 - 1150 nm. An example of a suitable unit would be ORIEL INSTA IV CCD SYSTEM 1024 x 128 with instaspec wedge flange, multispec spectrograph and grating assembly (Oriel model numbers 77118, 77439, 77400, 77415).

Computational equipment preferably comprises a computer 311 with at least the speed and storage capability of an IBM personal computer, Pentium with math co-processor, 10 gigabyte hard disk with tape back up drive, a National Instruments A/D converter card, LabView software for control, and Galatic Grams 32/Igor software for analysis. All data storage will preferably be done on a 105 megabyte removable cartridge type hard disk 312 (i.e. Sydos).

The present inventors have access to a pre-existing swine model for acute resuscitation under hyperbaric oxygen conditions using external cardiac massage. Measured parameters include EKG; EEG; arterial, mixed venous, and sagittal sinus blood gases; arterial, pulmonary arterial, pulmonary arterial wedge, mixed venous, and sagittal sinus pressures; mixed venous and sagittal sinus hemoglobin saturation by direct oximetry; cardiac output; core temperature; and expired gas. Presently, the animal is maintained for two hours after resuscitation during which time normal pressures and blood gases are maintained.

The model will require modification to include validation by NIRoscope measurements against cerebral PO_2 measurements taken by inserting an oxygen sensing electrode through a burr hole drilled in the skull. The model should also be extended to include a 72 hour chronic model.

Outcome indicators include:

1. Documentation of time of return of spontaneous circulation;
2. Normalization of arterial blood gases (ABG's);
3. Normalization of niroscopically determined cranial tissue PO_2;
4. Serial improvement in single photon emission computerized tomography (SPECT) brain scan by Ceretec® (technetium hexamethylpropyleneamine oxime (HMPAO)). Case work on injured and resuscitated divers indicates that Ceretec SPECT brain scanning elucidates perfusion/metabolism defects in the brain. (19).
5. Neurological function will be assessed using Canine Deficit Score.

To test the system and method of the present inventions, the following human studies will be conducted with proper informed consent from immediate family or custodial person with power of attorney.

Two groups of 20 human patients arriving in cardiopulmonary arrest at emergency departments with ongoing cardiopulmonary resuscitation and ACLS will be stabilized by an emergency department hyperbaric ACLS team. The patients will be randomized into two groups. Both groups will have the advantage of having hyperbaric environment modified Michigan Instrument automatic Thumper® and conventional ACLS pharmacology and ACLS algorithmic American Heart Association protocol. The subjects will be connected to a hyperbarically adapted volume cycled ventilator (10 mg/Kg for tidal volume) by endotracheal tube. Partial arterial pressure of carbon dioxide ($PaCO_2$) will be maintained at 40 mm Hg by the rate of ventilation. The control group will be brought to pressure of 4 fsw (1.22 msw - meters of sea water) and administered 100% O_2 by the endotracheal tube. The niroscope will record the cerebral cortex redox ratio of cytochrome aa_3. The treatment group will be initially administered 100% O_2, pressurized to minimum depths 60 fsw (18.3 msw). Once at 60 fsw (18.3 msw), both breathing gas mixture and chamber pressure will be controlled by the attending emergency physician using the output of the NIRoscope as a guide. Both groups will have cardiac monitoring by EKG and arterial continuous manometry by chart recorder. The patients post resuscitation, if successful, would have SPECT brain scan by Ceretec® HMPAO utilizing a dedicated Siemens triple head

high resolution radionuclide camera with three-dimensional computer reconstructed brain images to determine the extent of ischemia-induced brain damage and the presence of potentially recoverable brain tissue. Post-resuscitation treatment will include HBOT at 1.5 ATA (atmospheres absolute) twice a day for three days and once a day for four days. Outcome indicators will include numbers 1 through 4 used in the animal experiment above, as well as percentage of improvement in HBOT resuscitated patients. In addition, neurological function will be evaluated by a to-be-determined method.

The development of superior mathematical separation techniques was necessary because although the technology for small animals and neonates has been available, it has not successfully been applied to adults.

The NIRoscope is considered necessary for HBOT resuscitation. It would also be considered an invaluable tool for routine ACLS resuscitations at one atmosphere. Niroscopy will help to optimize treatments thereby limiting the exposure of patients and attending medical personnel to pressure environments greater than that which is necessary. Thus, it helps prevent patients from being exposed unnecessarily to too high pressures of oxygen while simultaneously helping to reduce the possibility of dysbaric incidents in the attending personnel. Any technology that informs physicians as to the efficacy of their resuscitation efforts would be extremely helpful. Three different authors are proposing to use tissue or blood oxygen content for helping to evaluate success of resuscitative efforts by physicians.

The NIRoscope 51 and 52 is shown in Figures 12 through 21 with the total NIRoscopic system shown in Figures 21 and 22. The system is composed of a stabilized near infrared (NIR) light source 100 (Figure 12) which includes a stabilized power supply 110, Quartz Tungsten Halogen light element 102, a parabolic light collector 111, a hot mirror 105 which eliminates visible and far infrared, and fiber optics light conduit 107. A band pass (600-1100nm) optical (special order from Oriel) filter can also be used. NIR light is transported via a fiber optics light conduit 216 and introduced into the patient's cranium by the pickup unit 200, 211. The pickup unit 200, 211 can be arranged in a single point mode (Figure 13) or for maximum NIR light delivery, a ring arrangement (Figures 14, 15, and 16) or without background correction (Figure 17, 18, or 19). Referring back again to Figure 21, NIR light is delivered to the pickup unit 211/230/250 by fiber optics light conduit 216 through the wall 24 of the chamber 20 to the light input optode 202, traverses through the scalp 205 (see Figure 13), skull 206, dura matter 207, pia

208, Arachnoid 209 and cerebral cortex 210, and back out again in reverse order via the NIR diffuse light path 212, 213. It has been theoretically predicted by Bonner and experimentally validated by McCormick that the depth of light penetration into the cranium is a function of optode spacing. An optode spacing of 5 cm has been found to be necessary to reach the cerebral cortex. Background pickup optode/ring 203 is located at a distance of approximately 3 cm. This distance is adequate to receive photons that have traversed the scalp and skull but not deep enough to reach the cerebral cortex. The sample pickup optode 204 is positioned to receive photons that have traversed the scalp, skull dura matter, and pia. Subtraction of the background signal from the sample signal results in only the signal representing the cerebral cortex. Absorption spectroscopy requires that the initial light source spectrum be subtracted from the measured light spectrum after traversing through the tissue. The source absorbance spectrum emanating from the cerebral cortex can be highlighted by subtracting any absorbance due to the overlying tissues (i.e., scalp, skull, etc.), from the spectrum measured at pickup optode 204. The spectrum from the signal pickup optode 204 and the background pickup optode 203 are routed to the dual wave interval spectrophotometer 300 by fiber optic conduits 218, 220 (Fig. 20). Both signals are received by a optical chopper 301 where they are presented to the charge-coupled device 307 in sequence via an aperture 304 and optical grading 306. It should be noted that electronic shutters (made by Newport model 845 HP) could replace the optical chopper of low light level applications where needed. The optical grading 306 spreads the spectrum out over the CCD in such a manner that the photon spectra is converted into an electronic spectra which is amplified by amplifier 308 and converted into a digital signal by A/D converter 309 and digitally stored by digital data storage unit 312. Proper sequencing and timing is performed by clock driver 315.

In memory digital data storage unit 312, two data streams are stored (i.e. sample and background spectra) (see Figure 23). Data storage unit 312 has available real time alternating background spectra 402 and real time alternating sample spectra 403. All noise pixels are corrected in all spectra 412 and smoothed by Sav-Golay smoothing function (2^{nd} degree polynomial with 51 points) 405. A difference absorption spectrum is then calculated 413 using each pair of background 402 and sample 403 spectrum. An example of calculated difference absorption spectrum 3 is shown in figure 1. Next, the dc component of the difference spectrum 3 is removed by integrating the spectrum 3 over the wave length span 400 to 1100 nm,

calculating the average wavelength adjustment by dividing the result of the integral by the wave length span interval, and then subtracting the resultant from each wave length absorbance value in the wave length span. An example of absorbance spectrum with DC component removed 5 is in figure 2. At this point the Fourier window 406 will be established. The Fourier window is the wave length interval about which the Fourier transform will be taken. It can be a general window which will separate each chromophore (i.e. oxidized and reduced cytochrome oxidase, oxyhemoglobin, deoxyhemoglobin, and water) into specific harmonic components, or a window for each chromophore can be established. At this point a Fourier transform 408 of the spectrum is computed resulting in values for each chromophore. As an alternate, Fourier deconvolution analysis 409 may be used if a more accurate indices of chromophore change is resulted. The resulting indices (for change in oxidized and reduced cytochrome oxidase, oxyhemoglobin and deoxyhemoglobin, and water) are stored 410 in data storage unit 312. These values may be displayed directly on monitor 313 as a function of time start of data acquisition or summed 411 and applied 460 to correct the cytochrome oxidase indices if the absorbance peaks are found to be interdependent.

An alternate simplified method shown in figure 24 is as follows. Rather than taking background spectra alternately with sample spectra, a single background spectrum is established before any sample spectrum is taken. Immediately after setup, a series of twenty spectra 418 are taken (for example with 6 second exposure and 4 second interval) and stored in data storage unit 312. Individual noise pixels are corrected 412. These twenty spectra are averaged 404 resulting in one average spectrum. The average spectrum is used as a constant background spectrum for the absorbance calculation of all subsequent sample spectra. All other steps remain the same as in Figure 23. This technique allow a less complicated arrangement as shown in Figure 8 verses the more complex arrangement shown in Figure 7.

All processing is preferably done in Pentium computer 311, with Galatic-Gram 32 software.

All of this equipment is commercially available in the form of a personal computer and a CCD spectrophotometer made by Oriel Inc.

All optical equipment used with the present invention is preferably from Oriel Inc. All control software is preferably from National Instrument and analytical software is preferably Grams 32 from Galatic and Igor. The computer is preferably a standard Pentium.

All measurements disclosed herein are at standard temperature and pressure, at sea level on Earth, unless indicated otherwise. All materials used or intended to be used in a human being are biocompatible, unless indicated otherwise.

APPENDIX OF REFERENCES

1. Virtis, M. Cost/Benefit analysis of cardiopulmonary resuscitation: a comprehensive study-Part II. Nursing Management 23(4):50-54, 1992.

2. Ebell, M. & Kruse, J. A proposed model for the cost of cardiopulmonary resuscitation. Medical Care 32(6):640-649, 1994.

3. Safar, P. Cerebral resuscitation after cardiac arrest: research initiatives and future directions. Ann of Emerg Med 22(2):2324-2349.

4. Holbach, L., et al. Differentiation between reversible and irreversible post-stroke changes in brain tissue: its relevance for cerebrovascular surgery. Surg Neurol, 7:325-331, 1977.

5. Iwatsuki, N., et al. Hyperbaric oxygen combined with nicardipine administration accelerates neurologic recovery after cerebral ischemia in a canine model. Critical Care Medicine, 22(5):858-863, 1994.

6. Van Meter, K., Gottlieb, S., & Whidden, S. Hyperbaric oxygen as an adjunct in ACLS on Guinea pigs after 15 minutes of cardiopulmonary arrest. Undersea Biomedical Research, 15(Suppl):55-56, 1988.

7. Neubauer, R., Gottlieb, S. Enhancing "idling neurons." Lancet 335:542, 1990.

8. Neubauer, R., Gottlieb, S., & Miale, A. Identification of hypometabolic areas in the brain using brain imaging and hyperbaric oxygen. Clinical Nuclear Medicine 17:477-481, 1992.

9. Neubauer, R. Gottlieb, S., Pevsner, H. Hyperbaric oxygen for treatment of closed head injury. Southern Medical Journal 84(9):933-936, 1994.

10. Waxman, K., Annas, C., Daughters, K., et al. A method to determine the adequacy of resuscitation using tissue oxygen monitoring. Journal of Trauma 36(6):852-857.

11. Rivers, E., Martin, G., et al. The clinical implications of continuous central venous oxygen saturation during human CPR. Annals of Emergency Medicine 21:1094-1101, 1992.

12. McCormick, P., Stewart, G., et al. Measurement of human hypothermic cerebral oxygen metabolism by transmission spectroscopy. Advances in experimental medicine and biology 333:33-41, 1993.

13. Jobsis, F., Piantadosi, G. et al. Near infrared monitoring of cerebral oxygen sufficiency. Neuro Resea 10:7-17, 1988.

14. Brazy, J. & Lewis, D. Changes in cerebral blood volume and cytochrome aa3 during hypertensive peaks in pre-term infarcts 108:983-987, 1986.

15. Glaister, D., Jobsis, F. A near infrared spectrophotometric method for studying brain O_2 sufficiency in man during + G_z acceleration. Aviation, Space and Environmental Medicine 59(3):199-207, 1988.

16. Cope, M. et al. System for long term measurement of cerebral blood and tissue oxygenation on newborn infants by near infrared translumination. Med and Biol Eng Comp 26:289-294, 1988.

17. Hoshi, Y. Et al. Oxygen dependence of redox state of copper in cytochrome oxidase in vitro. J App Phys 74(9):1622-1627, 1993.

18. Wray, S., et al. Characterization of near infrared absorption spectra of cytochrome aa3 and hemoglobin for the non-invasive monitoring of cerebral oxygenation, Bioch and Biophy Acta 933:918-929, 1987.

19. Adkisson GH, Hodgson M, Smith F, Torok Z, Macleon MA, Sykes JJW, Strack C, Pearson RR, Cerebral perfusion deficits in dysbaric illness, The Lancet, 2, 119-121, 1989.

20. Matcher S, Elwell C, Cooper E, Cope M, Delpy D. Performance comparison of several published tissue near-infrared spectroscopy algorithms. Analytical Biochemistry 1995; 227:54-68.

21. Miyake H., Nioda S., Zaman A., Smith D., Chance B. The detection of cytochrome oxidase, Heme Iron, and Copper Absorption in blood perfused and blood free brain in Normoxia and Hypoxia. Analytical Biochemistry 1991; 192:149-155.

Incorporated herein by reference is the paper entitled "Cytochrome oxidase reduction/oxidation charge coupled monitor with large area pickup optode" and reproduced on the following pages 30-43, which describes results of the invention of the present inventors applied to a swine model.

The foregoing embodiments are presented by way of example only; the scope of the present invention is to be limited only by the following claims.

Cytochrome oxidase reduction/oxidation charge coupled monitor with large area pickup optode

Frederick A. Kriedt[a,c], Cedric F. Walker[a], Harvey T. Swanson[b,c], Sheldon F. Gottlieb[c], Keith W. Van Meter[c]

[a]Department of Biomedical Engineering, Tulane University / New Orleans, LA 70118
[b]Department of Physiology, Tulane University School of Medicine / New Orleans, LA 70112
[c]Baromedical Research Institute, 3052 General Collins, New Orleans, La. 70114

ABSTRACT

Objective: Present primary methods for non-invasively monitoring cerebral cytochrome oxidase (aa_3) *in vivo* use small area pickup optodes (less than 10 mm^2), millisecond integration times, and discrete wavelengths. Measured and reported results of the methods remain controversial especially in human application. A new approach, using changes in instrument design applied to a pig model, may demonstrate more accurate results and feasibility in human application.

Methods: An instrument was designed to include a large area pickup optode (16.5 cm^2) with a liquid nitrogen cooled CCD type spectrophotometer using a 6 second integration period. The instrument was applied to a Swine (20-30 kg) model with 4.6 cm optode spacing. Procedure included reduction of aa_3 by substituting 100% oxygen breathing gas with 100% nitrogen and chemically reducing aa_3 by administering NaN_3 and KCN intravenously. Difference spectra (deoxygenated over time versus oxygenated) were computed.

Results: Except for amplitude, the near infrared spectra recorded through intact scalp and skull were identical to those from brain surface recordings. Reduction of scattering due to hypoxia was clearly evident in nitrogen induced spectra. Absorbance peaks, hemoglobin (Hb) (760 nm) and aa_3 (830 nm), were visible and did not seem to be affected by percentage of deoxyhemoglobin. The 600 nm peak is believed to be caused by scattering, not aa_3 absorbance. Work is continuing to further demonstrate the validity of the hemoglobin and aa_3 absorption peaks.

Keywords: Cytochrome oxidase, near infrared spectroscopy, hyperbaric, hypoxia, resuscitation

1. INTRODUCTION

Hyperbaric oxygen (HBO) therapy may have positive effects on the outcome after resuscitation following cardiopulmonary arrest (Van Meter 1985, 1999a, b, and c). Since excessive oxygen dosages can have detrimental effects (Neubauer, 1991, 1992, 1994), there is a need for a non-invasive method to determine adequate but not excessive oxygen dosage. The use of near-infrared (NIR) spectroscopy for non-invasively monitoring cerebral hypoxia, hemoglobin (Hb), and cytochrome oxidase (aa_3) was first proposed by Jobsis (1977) and later developed by Jobsis (1988), Cope (1988), Hazeki (1989), Piantadosi (1989), Ferrari (1990) and Wickramasinghe (1990). Monitoring Hb by NIR is widely accepted but is not suitable during HBO due to skewed results caused by excessive oxygenated Hb. Monitoring aa_3 is more promising but remains controversial in both utility and accuracy. Utility is questioned because the reduction of aa_3 does not occur until patients are in a very critical and perhaps irreversible hypoxic condition (Ferrari,1995 and Stingele, 1996). Following cardiopulmonary arrest, severe hypoxia exists. Utility does exist in this case because it is useful to determine

when and if severe cerebral hypoxia is mitigated as a result of resuscitation. The accuracy of measurements of change in reduction/oxidation (redox) ratio of aa_3 have also been questioned (Miyake 1991, Inagaki 1992, Mature 1995, Germon 1999). All present algorithms for evaluating the aa_3 redox ratio use mathematical models (based on Beer's law and independently measured extinction coefficients) and process values of absorbance measured at several discrete wavelengths (Mature 1995). Inaccurate measurements of extinction coefficients used in the application of Beer's law, and the non linearity of Beer's law, are some of the reasons alleged for the inaccuracy. We hypothesize that direct measurements (without mathematical models) in changes in the aa_3 absorbance peaks from continuous wave length spectroscopy (CWS) may be a more accurate method to determine change in aa_3 redox ratio. This study was a preliminary qualitative test of our approach.

2. METHODS

2.1 Animal preparation

Eight swine (20-25 kg) were anesthetized with 5% isoflurane in oxygen, and intubated while monitored by EKG (Medical Data Electronics Model 20401) and pulse oximeter (Nelcor Model N-100) attached to the ear. With exception to the nitrogen experiments, animals were maintained on 1-1/2 to 2% isoflurane in oxygen (expiratory pCO_2 between 35 and 40 mm of Hg) with a mechanical ventilator (Ohio Anesthesia) during the entire experiment. In the two nitrogen experiments, the isoflurane in oxygen was replaced with alpha chloralose (70mg/kg every eight hours) and merperidine (6mg/kg every 4 hours) administered intravenously (IV) while the animal continued to breathe 100% oxygen after completion of surgery. Femoral arterial and jugular venous cannulae were inserted. Body temperature was monitored with a rectal probe and maintained at 37° C with a warm water mat. In all experiments (invasive and non invasive), the optode was centered over the midline of the brain by placement in a bregmal scalp position and attached to the shaved head with a minimum of two bone screws placed through the scalp into the skull, rostral to the frontal lobe and caudal to the occipital region of the brain. For the invasive protocol, the dura mater was exposed by trephining a 6.5 cm diameter hole.

2.2 Instrumentation and recording

CWS (400-950 nm range) was conducted as follows. Light was provided by a 150 watt quartz-halogen lamp (Dolan Jenner 170 D) via a 1/16" solid fiber optics (36" long), through a ¼" columinator onto the tissue. Exiting light was collected in a 16.5 cm^2 semi circular area (centered 4.6 cm from light input), focused with a Fresnel lens into a condensor lens (columinator), through a 1/8" fiber optics bundle and into a liquid nitrogen cooled CCD spectrophotometer (ISA spectrograph model number CP140 with CCD-1024x256). All recorded spectra were processed with Grams 32 (Galactic Industries Corporation) software and stored digitally. Calibrated bandpass filters (Andover Corporation) were used to precisely mark reference wave lengths at 605, 760, 830, and 920 nm. The spectrograph was purposely chosen to be a low dispersion unit to allow identification of broad band absorption peaks as recommended by Keilin (1966).

2.3 Procedure for recording and processing spectra

The animals were allowed to stabilize (30 minutes) breathing 100% oxygen after all surgery. Reference spectra were then taken at 20 second intervals (6 second integration) for 6 minutes. Hypoxia was initiated by changing the breathing gas from 100% oxygen to 100% nitrogen. Sample spectra were taken at 50 second intervals (6 second integration) for a period of 45 minutes or longer. Difference absorbance spectra were calculated by computing the negative log (base ten) of the reference spectra divided by the sample spectra. After all absorbance computations were complete, high frequency noise was eliminated with a Sav-Golay smoothing function (Grams 32 sub routine) with a 2nd degree polynomial and 51 points. The Sav-Golay function was used because the spectral peaks under consideration are broad (low frequency) and will not be removed as the high frequency noise is eliminated. All spectra were taken *in vivo*.

The first series of spectra (invasive and non-invasive with pure nitrogen breathing gas causing hypoxia) were taken with and without the skull and scalp intact. For measurement of invasive spectra, the optode was centered on the hole and fixed to the skull with bone screws. The light input optode was positioned directly on the dura and the pickup optode focused on the 6.5 cm diameter semi circular area of dura mater whose area center was 4.6 cm from center of light input optode. The non-invasive series of spectra were taken with the optode located on the shaved scalp over the same section of brain.

Because it is believed that the 830 nm cytochrome oxidase peak is masked by deoxyhemoglobin (Ferrari 1995), a second series of non invasive spectra were taken. The optode was located on the scalp in a position identical to the non-invasive portion of the first series of spectra. The animal's cytochrome oxidase was chemically reduced with IV administered sodium azide (NaN_3) and potassium cyanide (KCN). Dosage of NaN_3 was 30 mg/kg or approximately 2.5 mM/liter of blood for the two animals. Dosages of KCN were 1.3 mg/kg or approximately 0.2mM/liter of blood for the first animal, 7.0 mg/kg or 1.0 mM/liter of blood for the second animal and 12.0 mg/kg or 1.6 mM/liter of blood for the last two animals. These chemicals bind the cytochrome oxidase and inhibit the extraction of oxygen from the blood, causing a large portion of Hb to remain oxygenated thereby reducing deoxyhemoglobin and its effect. Readings from the pulse oximeter were monitored to confirm the increase in Hb saturation. Due to the quick uptake of NaN_3 and KCN inhibitors, spectra were taken at 4 second intervals (6 second integration) for 16.6 minutes after the dose was given.

3. RESULTS

3.1 Measured spectra of invasive and non invasive experiments

The results of measured invasive and non-invasive spectra as a function of time due to general hypoxia can be seen in figure 1. Figure 1A shows invasive (skull and scalp removed) and figure 1B shows non-invasive (skull and scalp intact) results. Both figures 1A and 1B, each spectrum (b through i in figure 1A and b through h in 1B) was taken at sequential times after initiation of nitrogen breathing gas. As time increased each sequential spectrum represented the effect of an increase in hypoxia. Agreement in shape can be observed by comparing sequential spectrum in 1A against 1B but difference in the magnitude of absorbance is evident. In order to illustrate the similar shape of the two spectra, spectrum from each group (invasive and non-invasive) was plotted separately in figure 1C. These spectra were chosen from figures 1A and 1B 7 to 8 minutes after the heart stopped to be sure both were comparable and aa_3 was completely reduced.

3.2 Results of chemically reducing cytochrome oxidase

Two different cytochrome oxidase (aa_3) chemical reduction (inhibitor) experiments were conducted to identify whether the absorbance peak (800- 900 nm) is affected by deoxygenated Hb. Sodium azide and potassium cyanide were used to cause the cytochrome oxidase to reduce and blood hemoglobin to remain essentially fully saturated thereby removing the effect of deoxyhemeglobin.

3.2.1 Sodium azide experimental results

Figure 2 shows the results of two sodium azide infusions. Sodium azide was expected to bind with the aa_3 inhibiting the use of oxygen thereby preventing oxygen from being released from the hemoglobin. Furthermore, an increase in oxygenated Hb and a decrease in deoxygenated Hb should have resulted. Neither occured as evidenced by both the pulse oximeter and the 760 nm region of the spectra. Instead, both spectra a and b had Hb peaks at 760 nm. These results compare to pulse oximeter readings taken during spectral recording. After the sodium azide infusion, percent saturation dropped from 95% to 93% during experiment c whereas the pulse oximeter remained at 100% throughout experiment b. Spectrum c has a more pronounce deoxyhemoglobin peak at 760 nm than spectrum b which agree with the pulse oximeter results. There were other interesting features. When comparing spectra b and c in the 800 to 900 nm region, spectra c has a negative absorption peak (valley) which was not present in spectrum b. The reason for the difference is explained in section 4.2.

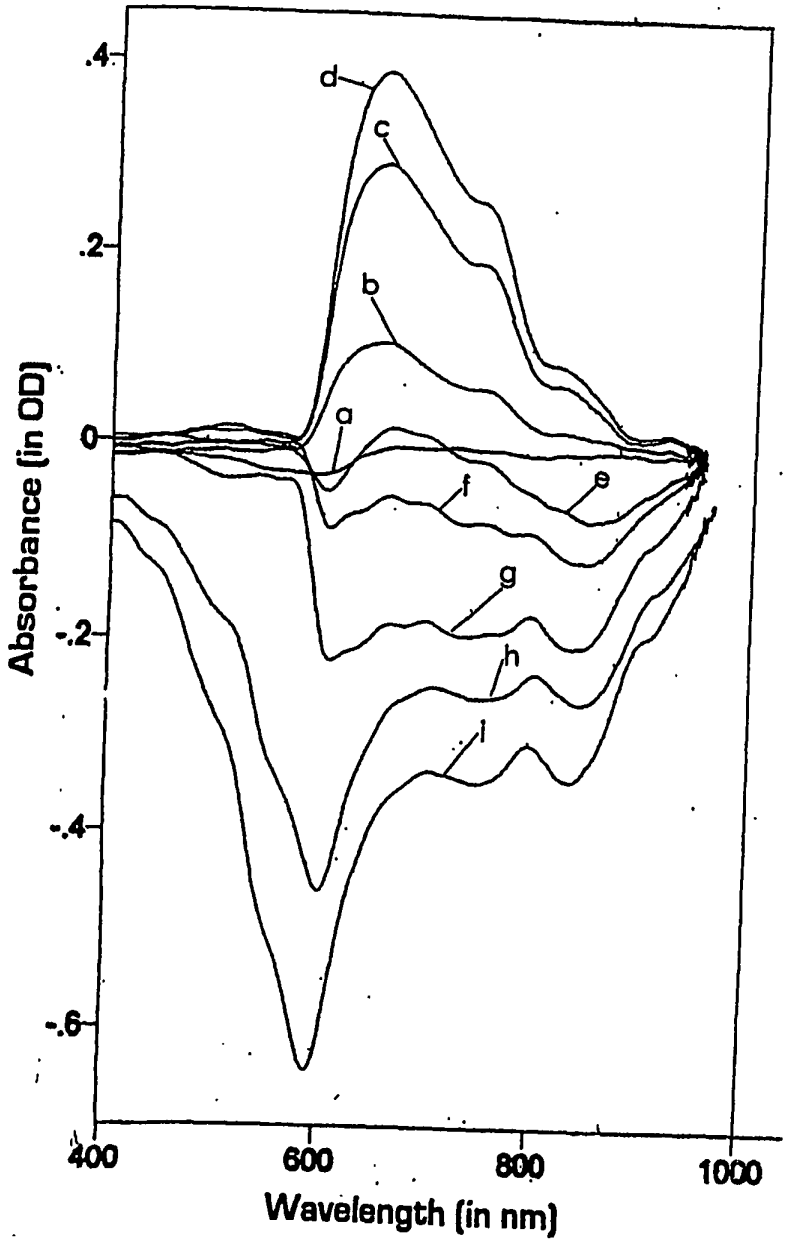

FIGURE 1A

INVASIVE EXPERIMENT

Difference absorption spectra from an exposed brain of a 23.0 kg swine.

100% oxygen is the reference. The samples are varying stages of hypoxia (caused by sequential time after breathing nitrogen).

Sequential times are as follows:

a - 0 seconds (100% oxygen);
b - 50 seconds;
c - 2 minutes 30 seconds;
d - 4 minutes 10 seconds;
e - 6 minutes 40 seconds;
f - 7 minutes 30 seconds;
g - 10 minutes 40 seconds;
h - 15 minutes 50 seconds;
i - 24 minutes 10 seconds.

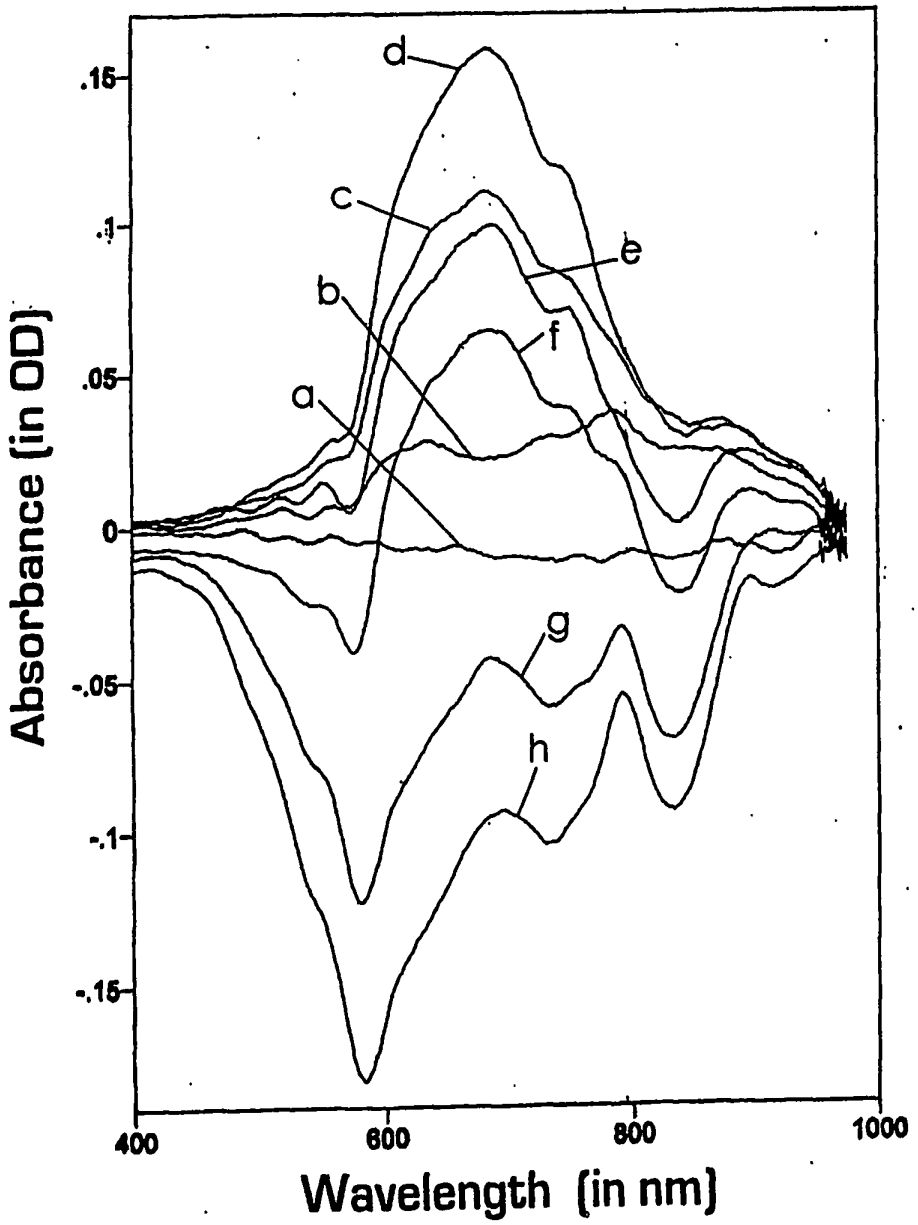

FIGURE 1B

NON-INVASIVE EXPERIMENT

Difference absorption spectra of the cerebral cortex taken from the scalp a of 24.3 kg swine.

100% oxygen is the reference. The samples are varying stages of hypoxia (caused by sequential time after breathing nitrogen).

Sequential times are as follows:
a - 0 seconds (100% oxygen);
b - 20 seconds;
c - 3 minutes;
d - 5 minutes 10 seconds;
e - 8 minutes 10 seconds;
f - 10 minutes 40 seconds;
g - 11 minutes 30 seconds;
h - 13 minutes 20 seconds.

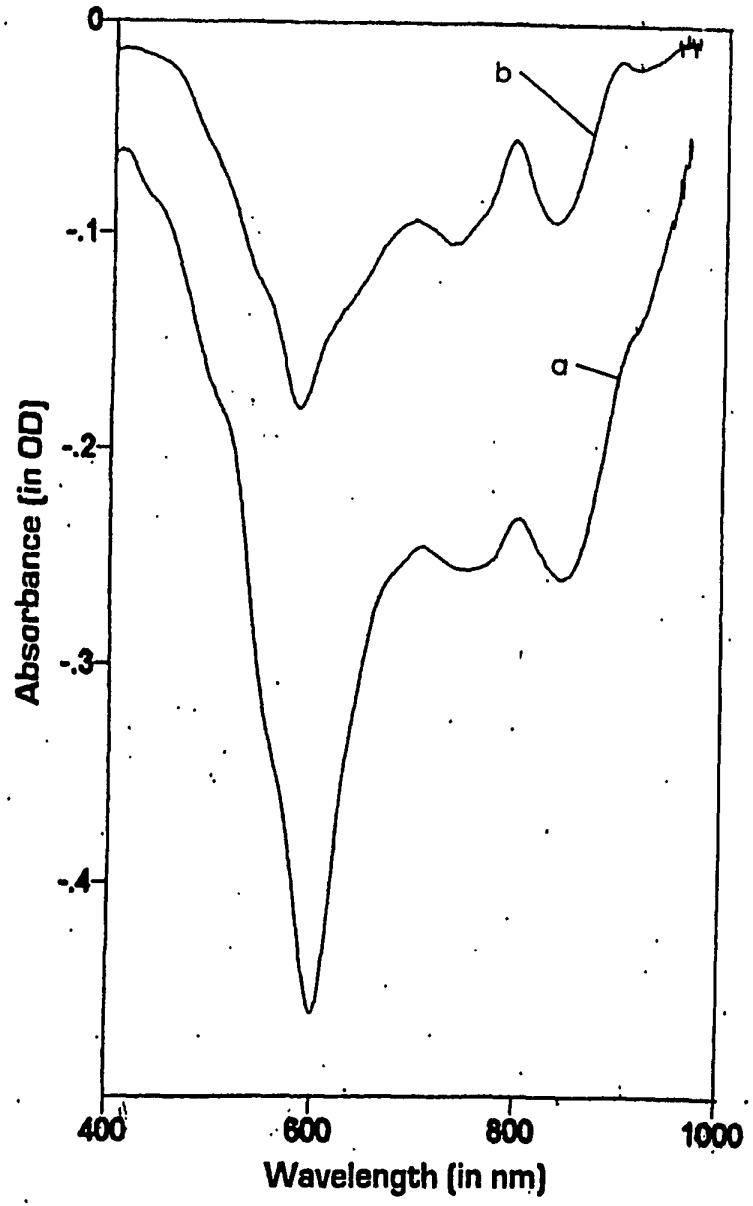

FIGURE 1C

COMPARISON OF SPECTRA FROM INVASIVE AND NON-INVASIVE EXPERIMENTS

Spectra are as follows:

a - spectrum from invasive experiment (directly on cerebral cortex) 8 minutes after cardiac arrest (from figure 1A curve h),

b - spectrum from non-invasive experiment (directly on scalp) 7 minutes after cardiac arrest (from figure 1B curve h).

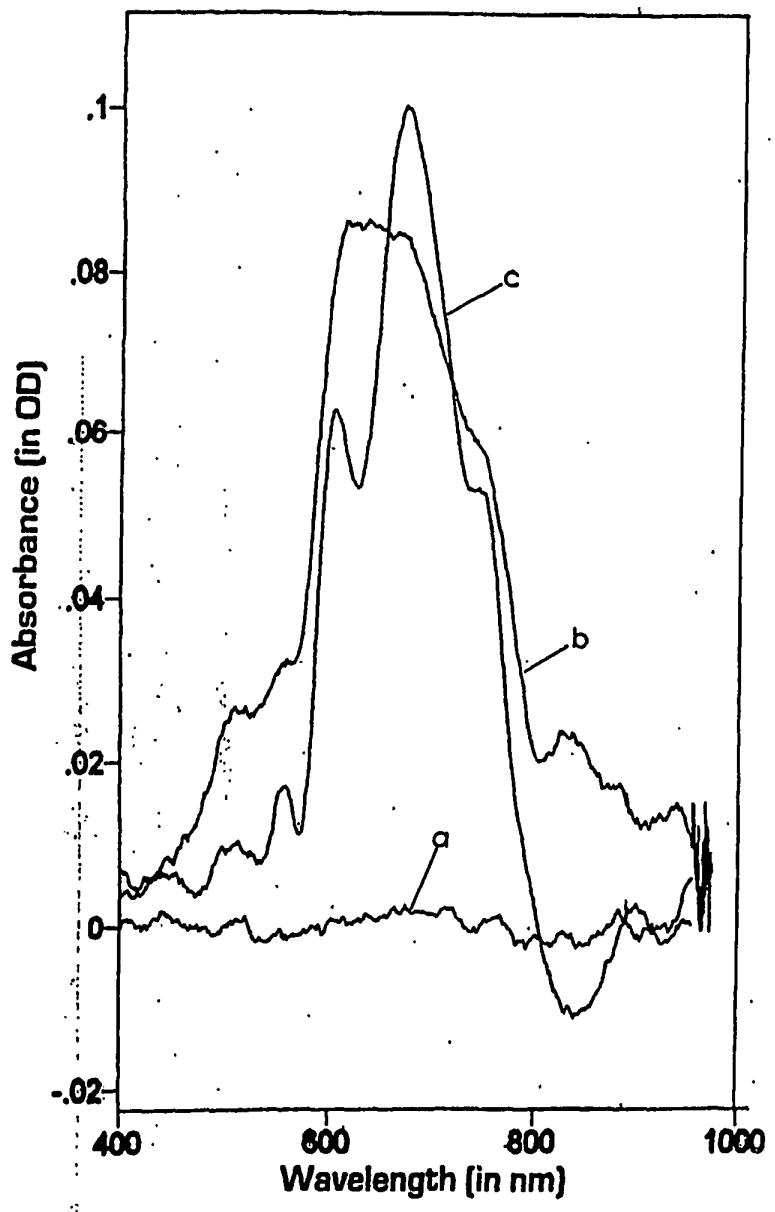

FIGURE 2

NaN_3 NON-INVASIVE EXPERIMENT

Difference absorption spectra of the cerebral cortex taken from the scalp.

100% oxygen is reference and sample is hypoxia after sodium azide infusion (30 mg/kg or approximately 2.5 mM blood concentration).

Spectra are as follows:

a - First animal: 100% oxygen (before infusion);

b - The first animal (25.5 kg). Concurrent to the time the spectra were taken the pulse oximeter remained at 100% saturation. Notice that the absorption peak at 800 to 900 nm is not present. During one hour and 5 minutes preceding the experiment the animal had a low blood pressure (60/40). It is believed that adequate blood perfusion of the brain did not exist resulting in a non viable aa_3.

c - The second animal (26.1 kg) resulted in peaks at 605 and 830 nm. Pulse oximeter registered 95% saturation before sodium azide infusion and 92% saturation after infusion.

PCT/US00/10968

3.2.2 Potassium cyanide experimental results

Because the sodium azide did not provide the expected results (increase in saturation), the experiments were repeated using potassium cyanide, a more aggressive inhibitor. Figure 3 shows the results from four different animals using three different concentrations of potassium cyanide. In all four experiments expected results did occur, namely the lack of a 760 nm peak in the absorbance spectra and no decrease in percent saturation on the pulse oximeter. Unfortunately, two new peaks appeared centered at 790 and 875 nm.

4. DISCUSSION

4.1 N_2 breathing invasive and non invasive experiments.

The first three sequential absorbance spectra (curves b, c, and d in figures 1 A and B) show an increase in all absorbances above 600 nm. After 7 to 8 minutes of N_2 breathing, the absorbance decreases (e through i in figure 1A and e through h in figure 1B) finally resulting in negative absorbance values. The units of absorbance are optical density. Optical density(OD) equals the negative log of reference intensity divided by sample intensity. Negative absorbance implies that the sample light intensity is greater than the reference intensity. We believe that an increase in sample intensity is the result of a decrease of brain tissue scattering. Reduction of scattering due to hypoxia which is believed to correlate with neuron depolarization has been documented by Federico (1994) and others. Further discussion of specific ranges of wavelength (600 nm, 600 to 750 nm, 760 nm and 800 to 900 nm) will follow.

4.1.1 600 nm negative peak

Initially the 600 nm negative peak (valley) was thought to be the 605 nm aa_3 heme absorbance band. But there are several factors which mitigate against this possibility. Absorbance is defined as the negative log of the reference light intensity divided by the sample intensity. In figure 2 of Griffiths' (1961) publication, the oxidized aa_3 absorbance peak at 605 nm is less than the reduced peak. These spectra are not difference spectra. Normal convention for recording spectra is to use water as the reference intensity. By definition of absorbance, this implies that the intensity of the oxidized aa_3 is greater than the intensity of the reduced aa_3. Therefore when changing the reference intensity from water to the oxidized condition (changing from conventional to difference spectrum), the peak should be positive (intensity of oxidized greater than the intensity of reduced) which it is not. In order to have a negative absorbance, the intensity of the reduced condition must be greater than the oxidized. Our only explanation of increased intensity during hypoxia is due to a decrease in scattering. We believe that the increased intensity is related to edema. Secondly, the 605 nm peak is in the wrong direction with respect to the 830 nm peak. They should be opposite in direction (605 nm should be a hill and 830 nm a valley). Finally, spectra using 100% nitrogen have a negative peak (see figure 1) at 605 nm whereas the chemical reduced spectra (NaN_3 /KCN, see figures 2 and 3) show a positive peak at 605 nm. Edema leading to reduced scattering is less likely to occur because the chemical hypoxic mechanism is very rapid. Therefore we believe that the 605 nm negative peak due to nitrogen induced hypoxia is caused by a reduction in scattering related to intra cellular edema (Federico, 1994), not a change in absorbance.

4.1.2 600 to 750 nm wavelength range

In figures 1A and 1B, spectra b, c and d show an initial increase in absorbance which follow the 800 nm Hb isobestic point. For this reason, we believe that the increase is due to growth in brain blood volume. Early increase in brain blood volume after a hypoxic insult has been reported by Kreisman(1985) and others. Notice also that the invasive peak (taken directly on the dura) is shifted to the right when compared to the non-invasive peak. Further study will be required to understand the right shift. Spectra e, f, g, and h show a decrease in absorbance. Curves e in both figure 1A and B generally agree with the onset of cardiac arrest

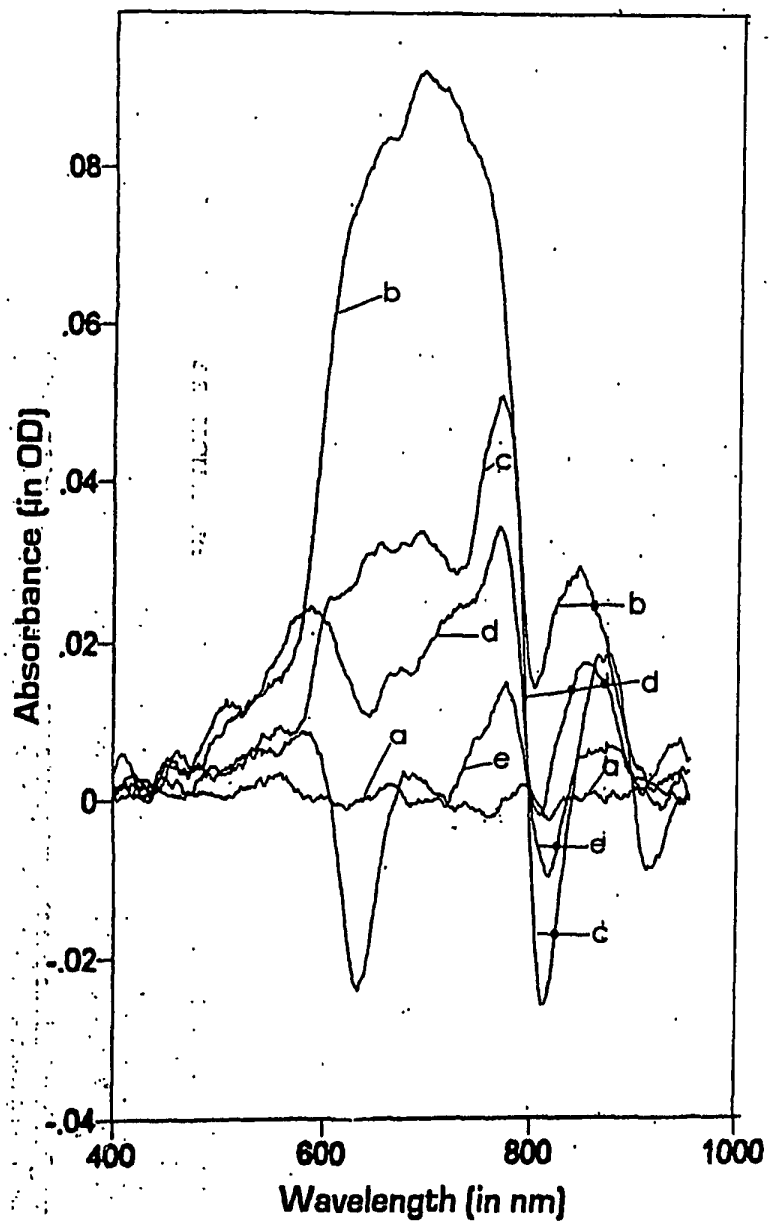

FIGURE 3

KCN NON-INVASIVE EXPERIMENTS

Difference absorption spectra of the cerebral cortex taken from the scalp.

100% oxygen is the reference. The samples are hypoxia after potassium cyanide infusion with three different concentrations into 4 pigs.

Spectra are as follows:
a - 100% oxygen (before infusion);
b - A 28.4 kg swine after infusion with 1.3 mg/kg or approximately 0.2 mM blood concentration;
c - A 27.4 kg swine after infusion with 7.0 mg/kg or approximately 1.0 mM blood concentration;
d and **e** - 26.5 and 30.5 kg swine after infusion with 12 mg/kg or approximately 1.6 mM of blood concentration.

In **b**, **c**, and **d** the pulse oximeter remained at 100% saturation throughout the experiment. In spectrum **c**, pulse oximeter read 93% saturation before infusion and 98% after infusion.

where blood volume will decrease. The continued decrease in absorbance of spectra f, g, and h cannot be explained by a reduction in blood pressure. Further work is necessary to understand this occurrence.

4.1.3 760 nm de-oxygenated Hb peak

The 760 nm peak is evident in spectra c, d, e, and f of both figures 1A and 1B, but seems to become obscure in curves f, g, h and i. At the same time a new absorbance positive peak develops at 790 nm. Further work is necessary to understand these occurrences.

4.1.4 800 to 900 nm negative absorbance peak

An absorbance peak in this region begins to develop in spectrum d of figure 1 B (non-invasive) and spectrum e in figure 1 A and continues to develop as hypoxia increases. The peak is centered approximately about 830 nm, and is in the correct direction (negative) but is not as broad as the 830 nm peak reported *in vitro* (Griffiths, 1961) and in bloodless rats and cats (Cope,1989, Miyake, 1991, and Stingele, 1996). Our peak extends from 800 to 900 nm rather than 750 to 950 nm as reported by the authors above. The difference between our results and all others is that there was blood in our optical field which was not present while the published spectra were taken. Further explanation of this difference in absorbance band width requires additional study.

Figure 1C is included to illustrate the similiarity of the invasive and non-invasive spectra. Location, number and direction of peaks are almost identical. This adds credibility to our assertion that spectra of the cerebral cortex can be distinguished non-invasively through the scalp and skull of a pig given a minimum optode separation distance of 4.6 cm. Minimal optode separation required to ensure passage of light through the brain remains a controversial subject (Germon, 1999).

4.2 NaN_3 results

These two experiments studied the effect of deoxyhemoglobin on the 800 to 900 nm absorbance band. We hoped the NaN_3 would block oxygen consumption therefore oxygen would remain bound to the hemoglobin. This should have resulted in oxygenated venous blood (100% saturation). If the change to 100% saturation correlated with a difference in the 800 to 900 nm spectral band as compared with nitrogen hypoxia, the difference would establish that deoxyhemoglobin has an effect. Unfortunately, pulse oximetry measured either no change or a decrease in saturation. This decrease rather than increase in saturation is substantiated by existence of the 760 nm deoxyhemoglobin peaks in spectra b and c of figure 2. We did notice that the 800 to 900 nm band was distinctively present in spectrum c and not present in spectrum b. After checking blood pressures during both experiments, we discovered that prior to taking any data in experiment b, the blood pressure remained at 60/30 for over an hour. We do not believe that the brain received adequate perfusion during that period at such a low blood pressure rendering the aa_3 non viable thereby resulting in no change in the 800 to 900 nm absorbance band. We included this tainted data because the results demonstrate the ability of this technique to distinguish viable from non viable brain tissue. Finally, the NaN_3 did not cause cardiac arrest. It was necessary to sacrifice the animal by introducing 100% nitrogen breathing gas. When the nitrogen was introduced, the pulse oximeter showed a drastic reduction in saturation(100% to 46%) with no change in the 800 to 900 absorption band. This result also implies that deoxyhemoglobin is not affecting the 800 to 900 nm absorbance band.

4.3 *KCN results*

Because the NaN_3 was not effective in reducing Hb saturation, we performed 4 experiments using a stronger inhibitor (KCN). Bernard (1856) first conducted this classic experiment. He found that when an animal breathed hydrocyanic acid, after the animal expired, the blood in both sides of the heart were red in color. The same results were duplicated in our experiments and can be found in figure 3. In all our KCN experiments, the Hb saturation remained at 100% or increased from 93 to 98%. In all KCN experiments the 760 nm absorbance band was not present. A positive absorbance peak did appear at approximately 790 nm,

but is different than the 760 nm peak as can be seen by comparing spectra a and b in figure 4. The 800 to 900 nm negative peak remained, although a new positive peak appeared to be superimposed at 850 to 925 nm, centered at 890 nm. This further indicates that the 800 to 850 nm peak is not being affected by deoxygenated Hb although further work must be done to identify the new peaks centered at 790 and 890 nm.

Figure 4 allows comparison of results of spectrum a, the result of NaN_3 infusion ; spectrum b, the result of KCN infusion; spectrum c, the result of hypoxia by 100% nitrogen breathing gas in a bloodless cat (Stingele,1996) and spectrum d, the result of hypoxia by 100% nitrogen breathing gas recorded non-invasively in a blood perfused pig. All spectra show an absorbance band in the 830 nm region which is believed to be the aa_3 NIR absorbance band. Spectra a and b clearly show that the 790 nm positive absorbance band is not the deoxygenated peak at 760 nm in spectrum a. When comparing spectra b, c, and d, all show a positive peak at 850 to 900 nm which may be water. Further studies will be necessary to confirm.

5.0 SUMMARY AND CONCLUSIONS

This study is preliminary and requires statistical verification and additional work. Although further study is necessary, the utility of using this technology is demonstrated. In the field of resuscitation, and especially hyperbaric resuscitation, NIR CWS can be used to determine whether administering oxygen to the aa_3 is causing a difference in the 800 to 900 nm wavelength range as resuscitation progresses. If no difference is measured in the aa_3 redox ratio, then the brain may not be viable indicating a possible irreversible brain injury. If changes in the 800 to 900 nm absorbance band do occur, they can be monitored until a steady state condition is established possibly indicating that the aa_3 now has an adequate supply of oxygen. Based on the preliminary data, we draw the following conclusions.

a.) Except for amplitude, difference absorption spectra of the cerebral cortex taken directly on the exposed brain (dura) versus through the scalp and skull are very similar at an optode spacing of 4.6 cm. This result adds to the validity of our hypothesis that the cerebral cortex can be monitored through the scalp and skull. (See figure 1A,B&C)

b.) A negative absorbance peak i.e valley, at 800-900 nm is clearly evident in all hypoxic experiments (N_2, NaN_3,&KCN). The amplitude of this peak correlates with the time after preventing or inhibiting oxygen from reacting with aa_3 (degree of hypoxia). It is narrower than published *in vitro and in vivo* peaks (i.e. reported to be 750 to 950 nm) and is suspected to be caused by a superimposed positive peak i.e. hill, of unknown origin at 850 to 900 nm (see all figures).

c.) The 800-850nm portion of the spectra is not affected by deoxyhemoglobin (see figures 2, 3, and 4)

d.) The possibility of using this method of determining adequate oxygen supply during HBO resuscitation has been demonstrated.

e.) The possibility of using this method to assess the viability of hypoxic cerebral tissue after reprofusion with oxygenated blood has been demonstrated.

f.) The effect of scattering due to hypoxia is clearly evident. The 605 nm negative peak is believed to be caused by artifact (probably scattering).

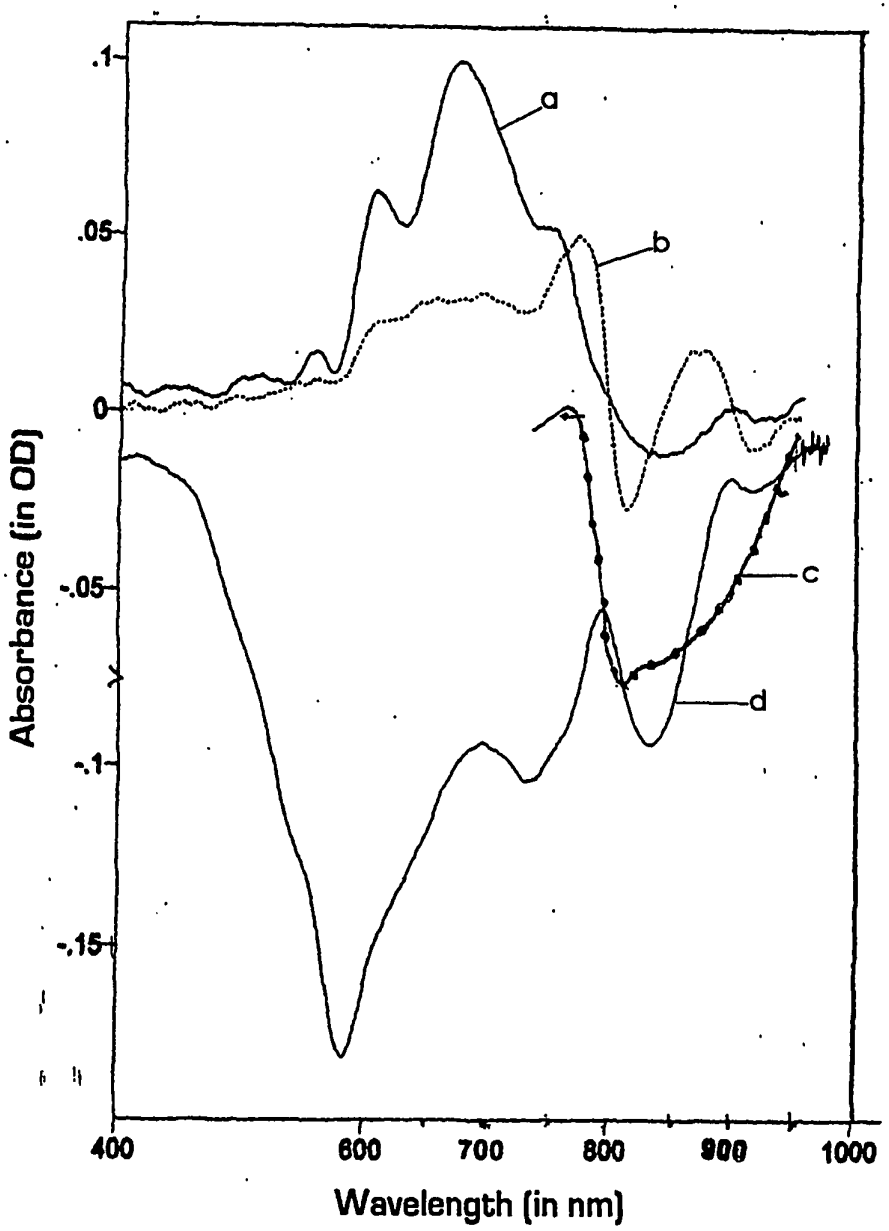

FIGURE 4

COMPARISON OF VARIOUS NON-INVASIVE HYPOXIC SPECTRA

Difference absorption spectra of the cerebral cortex taken from four different experiments.

Spectrum **a** is from NaN_3 experiment (from figure 2 spectrum c);

b is from KCN experiment (from figure 3 spectrum c);

c is taken from Stingele (1996) and is spectrum from a bloodless cat (perfluorocarbon substitute) with exposed skull (scalp and galea capitis and both temporal muscles retracted to expose the skull);

d is hypoxia due to nitrogen breathing gas (from figure 1b, spectrum h).

PCT/US00/10968

ACKNOWLEDGMENTS

The authors would like to thank Instruments SA Group for their grant in allowing the use of their CCD spectrophotometer.

REFERENCES

1. Bernard C. Lecons sur les effets des substances toxiques et medicamenteusus. Paris:Bailliere et Fils, 1857.
2. Cope M, Delpy D. System for long term measurement of cerebral blood and tissue oxygenation on new born infants by near infra-red transillumination. Med & Biol Comput 1988;26:289-294.
3. Federico P, Borg, SG, Salkauskus AG, MacVicar BA. Mapping patterns on neuronal activity and seizure propagation by imaging intrinsic optical signals in the isolated whole brain of the guinea-pig. Neuroscience 1994;58(3):461-480.
4. Ferrari M, Williams MA, Wilson DA, Thakor NV, Traystman RJ, Hanley DF. Cat brain cytochrome-c oxidase redox changes induced by hypoxia after blood-fluorocarbon exchange transfusion. Am J of Physiol. 1995;269(38) H4170-H424.
5. Ferrari M, Hanley DF, Wilson DA, Traystman RJ. Redox changes in cat brain cytochrome-c oxidase after blood fluorocarbon exchange. Am J Physio 1990;258:H1706-H1713.
6. Germon TJ, Evans PD, Barnett NJ, Wall P, Manara AR, Nelson,RJ. Cerebral near infrared spectroscopy: emitter-detector separation must be increased. British Journal of Anaesthesia 82(6) 1999:831-7.
7. Griffiths D, Wharton D. Studies of the electron transport system XXXV. Purification and properties of cytochrome oxidase. The Journal of Biological Chemistry 1961;236(6):1850-1856.
8. Hazeki D. Near infrared quadruple wavelength spectrophotometry of rat head. Adv in Ex Med and Biol. 1989;248:63-69.
9. Inagaki M, Tamura M. Brain oxygenation state: preparation of isolated perfused rat brain and near-infrared spectrophotometry. Adv in Ex Med and Biol. 1992;316:119-123.
10. Jobsis F, Kiezer J; LaManna J, Rosenthal M. Reflectance spectrophotometry of cytochrome aa_3 in vivo. J Appl Physiol 1977;43(5):858-852.
11. Jobsis F, Piantadosi C, Sylvia A, Lucas S, Keizer H. Near-infrared monitoring of cerebral oxygen sufficiency. Neuro Resea 1988;10:7-17.
12. Keilin D. *The History of Cell Respiration and Cytochrome,* Cambridge at the University Press, 1966, Chapter 8, page 152.
13. Kreisman N, Sick T, LaManna J, Rosenthal M. Local tissue oxygen tension-cytochrome aa_3 redox relationships in rat cerebral cortex in vivo. Brain Research. 1981;218:161-174.
14. Matcher S, Elwell C, Cooper E, Cope M, Delpy D. Performance comparison of several published tissue near-infrared spectroscopy algorithms. Analytical Biochemistry 1995;227:54-68.
15. Neubauer R, Gottlieb S. Stroke treatment. Lancet 1991; 337:1601.
16. Neubauer R, Gottlieb S, Miale A. Identification of hypometabolic areas in the brain using brain imaging and hyperbaric oxygen. Clin Nucl Med 1992;17;447-481.
17. Neubauer R, Gottlieb S, Pevsner N. Hyperbaric oxygen therapy in closed head injury. Southern Medical Journal 1994;87:933-936.
18. Piantadosi C. Behavior of the copper band of cytochrome c oxidase in rat brain during FC-43 for blood substitution. Adv in Ex Med and Biol 1989;248:81-90.
19. Stingele R, Wagner B, Kameneva MV, William MA, Wilson DA, Thakor NV, Traystman RJ, Hanley DF. Reduction of cytochrome-c oxidase precedes failing cerebral O_2 utilization in fluorocarbon-perfused cats. Am. J. Physiol 1996; 271(Heart Circ. Physiol.40) H579-H587.
20. Van Meter K, Gottlieb S, Whidden S. Hyperbaric oxygen as an adjunct in ACLS on guinea pigs after 15 minutes of cardiopulmonary arrest. Undersea Biomedical Research. 1988;15(Suppl)55-56.
21. Van Meter K, Sheps S, Swanson H, Wilson J, Barratt D, Kodu E, Roycraft E, Moises J, Nolan T, Harch P. Procine open chest cardiopulmonary resuscitation of swine in a controlled, prospective randomized trial incorporating normobaric and hyperbaric oxygen after a prolonged normothermic cardiopulmonary arrest. Undersea & Hyperbaric Medicine, 1999;26(Suppl):72.

22. Van Meter K, Sheps S, Swanson H, Wilson J, Barratt D, Kodu U, Roycraft L, Moises J, Harch P. A controlled prospective randomized pilot open chest cardiopulmonary resuscitation (CPR) comparing use of 100% oxygen in mechanical ventilation of swine at one, two and four atmospheres ambient pressure after a 25 minute normothermic cardiopulmonary arrest at one atmosphere. Journal of Academic Emergency Medicine, 1999;6(5):428.
23. Van Meter K, Swanson H, Sheps S, Barratt D, Roycraft E, Moises J, Kileen J, Harch P. Oxygen dose response in open chest ACLS in swine after a 25-minute cardiopulmonary arrest. Annals of Emergency Medicine 1999; 34(4):S11.
24. Wickramasinghe Y, Rolfe P. NIR procedures for monitoring hemoglobin and cytochrome oxidase in rat brain. EC Biomed Newslett. 1993;2(5).